Relaxor ferroelectric characteristics and temperature-dependent domain structure in a (110)-cut $(PbMg_{1/3}Nb_{2/3}O_3)_{0.75}(PbTiO_3)_{0.25}$ single crystal

X. Zhao, J. Y. Dai,* J. Wang, H. L. W. Chan, and C. L. Choy
Department of Applied Physics, The Hong Kong Polytechnic University, Hung Hom, Kowloon, Hong Kong, People's Republic of China

X. M. Wan and H. S. Luo
State Key Laboratory of High Performance Ceramics and Superfine Microstructure, Shanghai Institute of Ceramics, Chinese Academy of Science, 215 Chengbei Road, Jiading, Shanghai 201800, People's Republic of China
(Received 15 November 2004; published 23 August 2005)

Relaxor ferroelectric characteristics of (110)-cut $(PbMg_{1/3}Nb_{2/3}O_3)_{0.75}(PbTiO_3)_{0.25}$ single crystal has been revealed by temperature-dependent hysteresis loops and dielectric permittivities measurements. Ferroelectric domain structure and evolution in the as-grown and the poled samples have also been studied by means of temperature-dependent piezoresponse force microscopy. The result from the as-grown single crystal reveals that the microdomain size distribution follows an exponential cutoff, and the crystal exhibits a transition from ferroelectric microdomain to paraelectric phase upon heating; while being cooled back to room temperature, new microdomains are rebuilt. By contrast, lamellar-shaped macrodomains have been observed in the poled sample and transitions from macro- to microdomain structures at 90 °C and from microdomain structure to paraelectric phase at 115 °C have been observed upon heating, respectively.

DOI: 10.1103/PhysRevB.72.064114 PACS number(s): 77.84.−s, 68.37.Ps, 77.80.Dj, 77.65.−j

I. INTRODUCTION

Relaxors, such as $Pb(Zn_{1/3}Nb_{2/3})O_3$ (PZN) and $Pb(Mg_{1/3}Nb_{2/3})O_3$ (PMN), have the main features of significant frequency dependence of their peak relative permittivities, the absence of macroscopic spontaneous polarization, and persistence of the local polarization far above the transition temperature.[1] Relaxors are commonly thought to be complex perovskites with ABO_3 type cell unit and characterized by the ionic disorder resulted from the randomly occupation of the B site by at least two different valence cations.[1–3] In the case of PMN, one of the typical relaxors, these two valence cations are Mg^{2+} and Nb^{5+}. By doping the $PbTiO_3$ (PT) in the PMN, the solid solutions of $(Pb(Mg_{1/3}Nb_{2/3})O_3)_{1-x}(PbTiO_3)_x$ (PMN-PT) can be obtained, and the substitution of B site ions with ferroelectrically active Ti^{4+} can cause the PMN-PT a gradual transformation from relaxor ferroelectrics to normal ferroelectrics.[4] Due to the superior dielectric and electromechanical properties, relaxor ferroelectrics are considered the best piezoelectric materials in the new-generation of transducers, sensors, and actuators,[5–7] and intensive research effort has been given to fundamental understanding of the structural and physical properties.

It is widely accepted that the properties of relaxor ferroelectrics can be described in terms of the formation of polar nanosized regions (PNRs), which are found to form at the so-called Burns temperature and persist below transition temperature.[1,8,9] Gehring and Shirane *et al.* reported in their work the "waterfall" anomaly in the transverse optic (TO) phonon observation of PT doped PMN and PZN, and PNRs have been attributed as the cause of the damping due to their random polar nature.[10–12] Blinc and co-workers also proposed a spherical random-bond-random-field (SRBRF) model of dipolar glasses based on polar cluster interacting to describe the local polarization and nonlinear dielectric susceptibility in PMN.[13,14]

The PMN-PT single crystals are believed to have a morphotropic phase boundary (MPB) in the range of 28%–36% of PT. When PT% $>$ 36%, the PMN-PT single crystals behave as normal ferroelectrics, where only macrodomains with sizes of hundreds of microns exists. On the other hand, when PT% $<$ 28%, only rhombohedral microdomains exist in the single crystals; while if poled by an external electric field, these microdomains can be transformed to macrodomains.[15–18] The relaxor characteristics of poled PMN-PT can be revealed by two temperatures T_d and T_m, where T_d is the transition temperature from the macrodomain to the microdomain and T_m represents the phase change temperature from the ferroelectric to paraelectric phases.[15–18] The domain evolution in relaxor PMN-PT single crystals can be regards as a transition from nanodomain to microdomain and macrodomain.

Because of its important role in the relaxor phenomenon, the evolution of domain structures in relaxor ferroelectrics under different temperatures and electric fields have attracted a great deal of interest in recent years. In early studies, the results were mainly obtained from indirect information such as temperature dependence of relative permittivity or high-energy x-ray diffraction and neutron diffraction.[3,7,19] Optical methods were commonly used to visualize domain structures. Tu *et al.* studied the evolution of domain structures in PMN-PT single crystals under zero-field-heating (ZFH) and field-cooling-zero-field-heating (FC-ZFH) using a polarized microscope.[20–23] However, limited by the resolution, the optical method is appropriate only for observing domains of a size in the order of microns, and is focused on the compositions with a PT% of close to 35%, which exhibit micron-sized domain structures at room temperature.[20–24]

After the piezoresponse force microscopy (PFM) was successfully applied to the study of ferroelectric materials in the

nanometer scale, the situation improved a great deal. Several studies on the direct observation of domain structures in relaxor ferroelectrics have been reported, with the resolution approaching the scale of nanometers.[25–27] Very recently, Shvartsman and Kholkin reported a complex polar structure with nanometer sizes, which reflects the appearance of the ferroelectric state at room temperature and the existence of PNRs in a large temperature range.[26] Nevertheless, the attempts have not been enough to achieve an understanding of relaxor ferroelectrics such as the domain evolution under varied temperatures after poling at room temperature and the microdomain-macrodomain transition induced by varying the temperature. In this work, we reported the domain evolution observed in both as-grown and poled rhombohedral PMN-PT single crystals.

II. EXPERIMENT

The PMN-25PT single crystal was synthesized by the modified Bridgman technique and the major faces were cleaved as normal to the ⟨110⟩ direction.[24] Here, the direction "⟨110⟩" refers to the pseudocubic axes, and hereafter the single crystal cut perpendicular to this direction is called "(110)-cut" single crystal. Samples for measurement are plates with areas of $2-3\times 5$ mm^2 and thickness of 1 mm. For measurements of the temperature dependence of hysteresis loops (P-E loops) and dielectric permittivity ($\varepsilon' \sim T$), Au was coated on both sides as electrodes. In order to determine the domain evolution in the as-grown and poled single crystal, one sample was poled along the ⟨110⟩ direction by an electric field of 4.5 kV/cm at 70 °C for 15 min, and of 2.25 kV/cm in the process of cooling the sample down to room temperature. The temperature dependence of the hysteresis characteristics of the (110)-cut PMN-25PT single crystal was measured using a Sawyer-Tower circuit at the temperature from room temperature (denoted as 25 °C) to 140 °C, which is much higher than the T_m. Using an impedance analyzer (HP4194A) equipped with a temperature chamber (Delta 9023), the temperature dependence of the relative permittivities of the as-grown and the poled single crystal was measured at temperatures of 40–240 °C at frequencies of 100, 1 k, and 10 kHz.

For the PFM characterization of domain structure, the as-grown and poled samples were mechanically polished to a thickness of about 15 μm and a PFM (Nanoscope IV, Digital Instruments) utilizing a conductive tip coated with Pt was carried out. In the experiments, the tip was electrically grounded, while a modulating voltage of 6 V (peak-to-peak) with 11 kHz was applied on the bottom electrode.

III. RESULTS AND DISCUSSION

The P-E loops obtained at different temperatures are shown in Fig. 1, where a rather good typical hysteresis characteristic for the (110)-cut PMN-25PT single crystal can be seen at room temperature (25 °C). The remnant polarization (P_r) is measured to be 32.0 μC/cm^2, which is very close to the value of the saturation polarization (P_s); and the coercive electric field (E_c) is also determined to be 2.6 kV/cm from

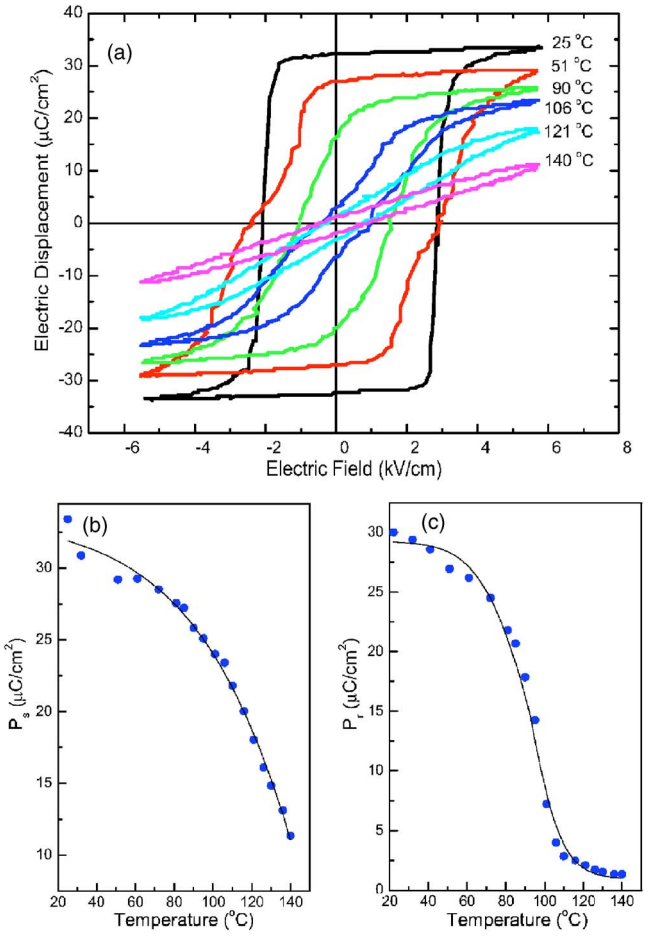

FIG. 1. (Color online) Temperature dependence of (a) hysteresis loops, (b) saturation polarization (P_s), and (c) remnant polarization (P_r).

the P-E loop at room temperature. The temperature dependence of the P_s and P_r can be revealed from the temperature-dependent P-E loops, as shown in Figs. 1(b) and 1(c). It can be seen that, when the temperature rises to 90 °C, the P_s decreases by 31% to a value of 22 μC/cm^2, while P_r decreases by 53% to 15 μC/cm^2. The P_r decreases much faster than the P_s as the temperature rises, and at 140 °C the P_r is close to zero. It should be noted that when the temperature reaches 140 °C, which is well above the T_m, the hysteresis characteristics can still be identified from the P-E loop, where the P_r is nonzero although it is very close to zero. This suggests that the microdomains still exist at temperatures much higher than T_m in the PMN-25PT single crystal. The features of a large P_r, the slow decrease of P_s and nonzero P_r at high temperatures, are characteristics of relaxor ferroelectrics and an explanation for these features in terms of a microdomain-macrodomain transition has been given.[5,18,28]

The temperature-dependent relative permittivities of the as-grown and the poled PMN-25PT single crystals upon heating and cooling are shown in Fig. 2. Relaxor ferroelectricity is apparent as illustrated in Fig. 2(a), where the T_m is determined to be 115 °C at 1 kHz. Corresponding to the empirical equation,

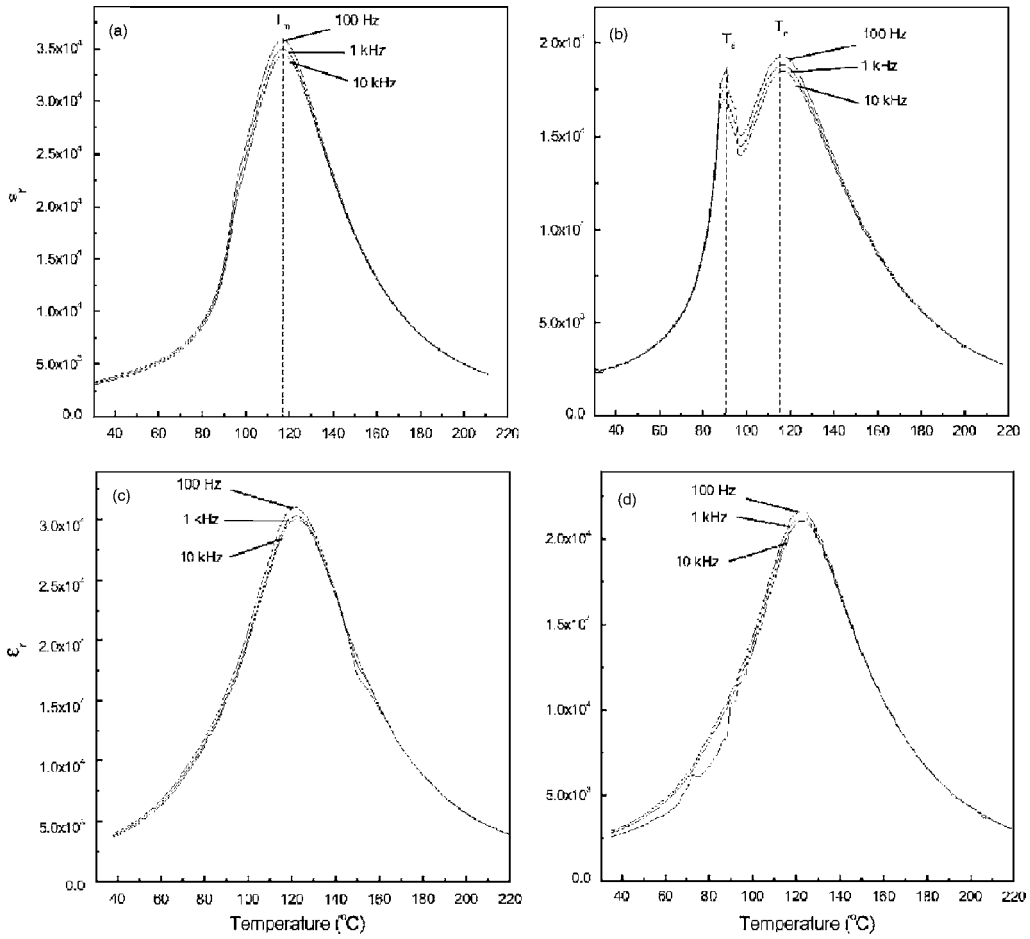

FIG. 2. Temperature dependence of relative permittivity ($\varepsilon' \sim T$) for the (110)-cut PMN-25PT single crystal upon heating of (a) the as-grown and (b) the poled samples; and upon cooling of (c) the as-grown and (d) the poled samples.

$$T_m = 5x - 10, \tag{1}$$

where x represents the composition of PT, the single crystal can be confirmed to be PMN-25PT.[29,30] Upon heating, the temperature dependence of relative permittivities for the as-grown and the poled sample are shown in Figs. 2(a) and 2(b). Fig. 2(b) also reveals a transition temperature at T_d=90 °C, where the dispersion feature for different frequencies at $T > T_d$ suggests a macrodomain-to-microdomain transition in the poled sample. In contrast, there is only a small shoulder at 90 °C for the as-grown sample, indicating that the microdomain structure is dominant. Figures 2(c) and 2(d) represent the temperature dependence of relative permittivity for the PMN-25PT single crystals upon cooling, where almost the same curve as heating can be observed. It can be concluded that, without an external electric field, only a microdomain exists when the sample is cooled down from the paraelectric phase no matter whether the sample has been poled or not before heating.

Figure 3 shows the piezoresponse images of the as-grown and the poled (110)-cut PMN-25PT single crystal at room temperature. It can be seen from Fig. 3(a) that speckle-shaped domains, with sizes varying from the maximum of 8 μm^2 to less than 100 nm^2, are the dominant domains in the as-grown sample at room temperature. In contrast to the

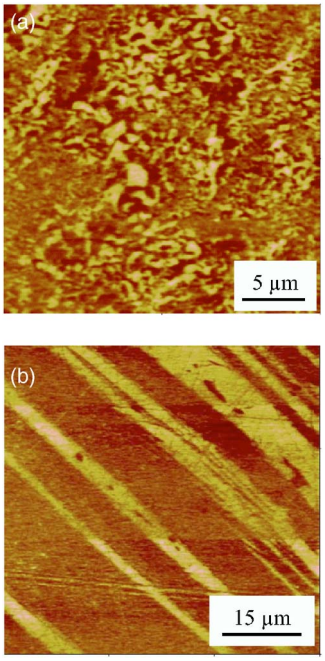

FIG. 3. (Color online) Domain structure at room temperature in (a) the as-grown and (b) the poled (110)-cut PMN-25PT single crystal.

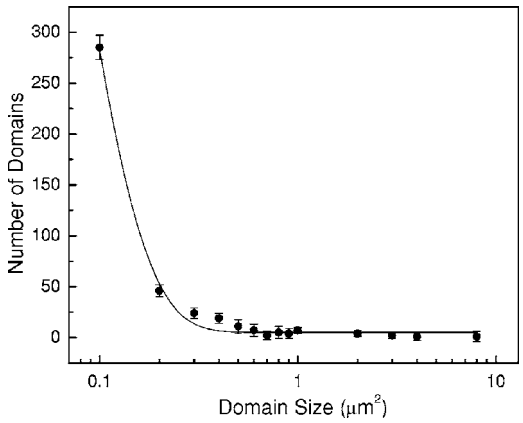

FIG. 4. Domain size distribution of the as-grown (110)-cut PMN-25PT single crystal.

speckle-shaped domains in the as-grown sample, stripe-shaped domains are found to exist in the poled sample as shown in Fig. 3(b). The widths of the stripes vary from several to 10 μm, which are much larger than the diameter of the speckle-shaped microdomains in the as-grown sample. It is apparent that, in the poled sample, microdomains have been transformed to macrodomains due to the applied external electric field.[5] Based on the experimental condition, the regions with "black" contrast in Fig. 3(b) correspond to the macrodomains formed by the poling process, and the "white" contrast regions are believed to be the domains that have not been successfully poled or the domains that have been depolarized. The stripe shape of the domains is consistent with the reported optical observations of the macrodomains.[24]

Based on Lehnen and Shvartsman's results on $Sr_{0.61-x}Ce_xBa_{0.39}Nb_2O_6$ (SBN61: Ce) and PMN-20PT single crystals,[26,27] the relaxor properties can be well described using 2D random-field Ising model (RFIM). The domain size distribution in relaxor ferroelectrics is believed to follow a power law with an exponential cutoff as follows:

$$N_d(S_d) \sim S_d^{-\delta} \exp\left(-\frac{S_d}{S_0}\right), \tag{2}$$

where N_d is the number of domains of the size of S_d, and S_0 is the upper cutoff of the domain size. Figure 4 shows the relationship between the domain number and the domain size of the as-grown (110)-cut PMN-25PT single crystal. The data were collected by the analysis function of the DI software (Digital Instruments). Each value is the average of 3–5 times' collections, and the statistical error has been given in the curve. The experimentally observed domain sizes in our sample can also fit well with Eq. (2), and the best fit yields the value of exponent δ as being 2.41 and S_0 as being 1.30 μm^2. As described by Shvartsman, δ corresponds to a big variation of the domain size.[26]

Figure 5 shows piezoresponse images of the as-grown sample at different temperatures. During heating, it can be seen that the contrast between the oppositely polarized domains decreases and the boundaries of the domains become rougher [Figs. 5(b)–5(d)], while there is little change in the shape and number of domains. Some microdomains can still

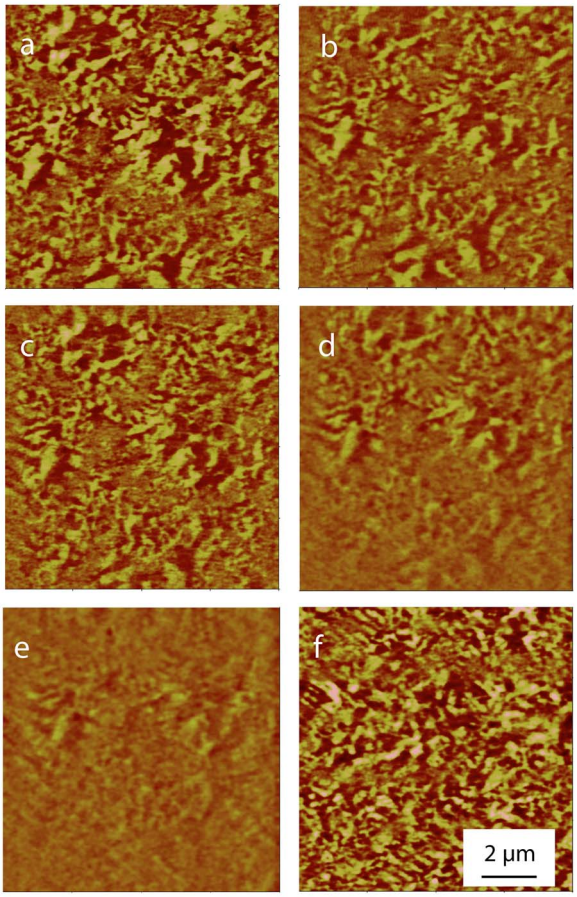

FIG. 5. (Color online) Temperature-dependent piezoresponse images showing the domain evolution of the as-grown (110)-cut PMN-25PT single crystal at (a) 25, (b) 80, (c) 110, (d) 120, and (e) 150 °C. (f) Piezoresponse image after the sample was cooled back to room temperature.

be seen when the temperature is above the transition temperature, T_m. At 150 °C, however, most of the domains disappear [Fig. 5(e)]. After the sample has been cooled down to room temperature, the microdomain structure appears in the same region again, as shown in Fig. 5(f). This domain structure evolution is consistent with the temperature-dependent relative permittivity measurement as shown in Fig. 2. It should be noted, however, that when the sample has been cooled back to the room temperature, the same area presents a different domain pattern than that prior to heating. The different domain structure after heating and cooling process is believed to be due to the random fields in the single crystal during cooling process.

The temperature dependence of the domain density, average piezoresponse amplitude, and sum of the domain areas are shown in Fig. 6. It can be seen that the sum of the domain areas and the domain density change very little at lower temperatures. However, when the sample is heated to a temperature near the transition temperature, T_m, both the domain density and the sum of the domain areas decrease quickly, but they do not become zero even when the temperature is well above T_m. The residual domains are believed to be those that contain PNRs which can exist at temperatures well

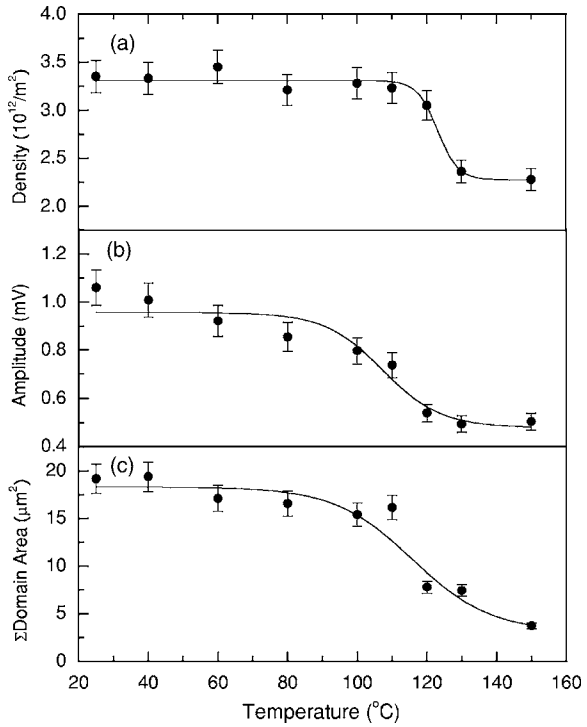

FIG. 6. Temperature dependence of (a) the domain density, (b) the average amplitude of the piezoresponse, and (c) the sum of the domain areas of the as-grown (110)-cut PMN-25PT single crystal.

above T_m.[11,26,31] On the other hand, the average piezoresponse amplitude has a similar change as the P_r, which decreases continuously to a value close to zero. The nonzero amplitude at high temperature reveals that the polarization persists in a broad temperature range due to the existence of PNRs.

Figure 7 shows the evolution of the temperature-dependent domain structure in the poled (110)-cut PMN-25PT single crystal, where (a)–(f) correspond to the domain images at 25, 90, 100, 110, 120, and 140 °C upon heating, respectively. All of the piezoresponse images in Fig. 7 were obtained from the same region. However, compared to Fig. 3(b), which is from another region in the same sample, the stripe-shaped macrodomains shown in Fig. 7(a) are not very uniform. It can be seen that at room temperature the domain walls are smooth and the contrast is sharp. In the temperature range from room temperature to 90 °C, there is no significant change in the size and shape of the domains. However, as shown in Fig. 7(b), when the temperature reaches 90 °C, the sizes of the "white" speckles and stripes increase, and some new speckles appear. At 100 °C, as shown in Fig. 7(c), more "white" speckles with diameter of less than 100 nm appear, and one can see that the sizes of the speckles and stripes keep on increasing. When the temperature reaches 110 °C, it is also apparent that the contrast of the stripe-shaped domain becomes weaker, and some stripe-shaped domains disappear; while the diameters of the newly appeared speckle-shaped domains increased to several hundred nanometers [Fig. 7(d)]. The domain structure continues to change as the temperature increases. When the temperature surpasses T_m, reaching 120 °C, the contrast of the piezoresponse image becomes much weaker and the domain walls become rather blurred [Fig. 7(e)]. At a temperature of 140 °C, which is well above the T_m, no obvious domain structure can be identified in the piezoresponse image [Fig. 7(f)], where a gray contrast dominates the image, except for a few "black" and "white" dots that may correspond to the normal ferroelectric domains of $PbTiO_3$ or to defective pinned domains. When the sample was cooled down to room temperature, at the same region, no stripe-shaped macrodomain could be seen from the piezoresponse image, except for some speckle-shaped domains with sizes smaller than 1 μm [Fig. 7(g)]. Therefore, it can be concluded that without an external field no macrodomain can be formed during cooling. In order to have a comparison with the domain pattern of the as-grown sample after being cooled back to room tem-

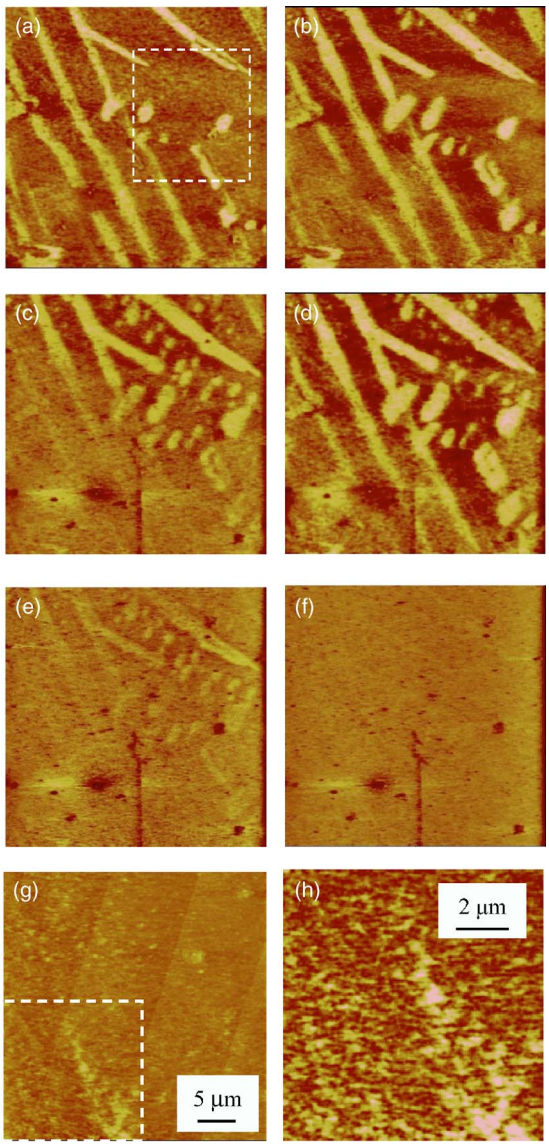

FIG. 7. (Color online) Temperature-dependent piezoresponse images of domain evolution in the poled (110)-cut PMN-25PT single crystal upon heating: (a) 25; (b) 90; (c) 100; (d) 110; (e) 120; and (f) 140 °C. (g) Piezoresponse image after the sample was cooled back to the room temperature. (h) The magnified domain image of the outlined region in (g).

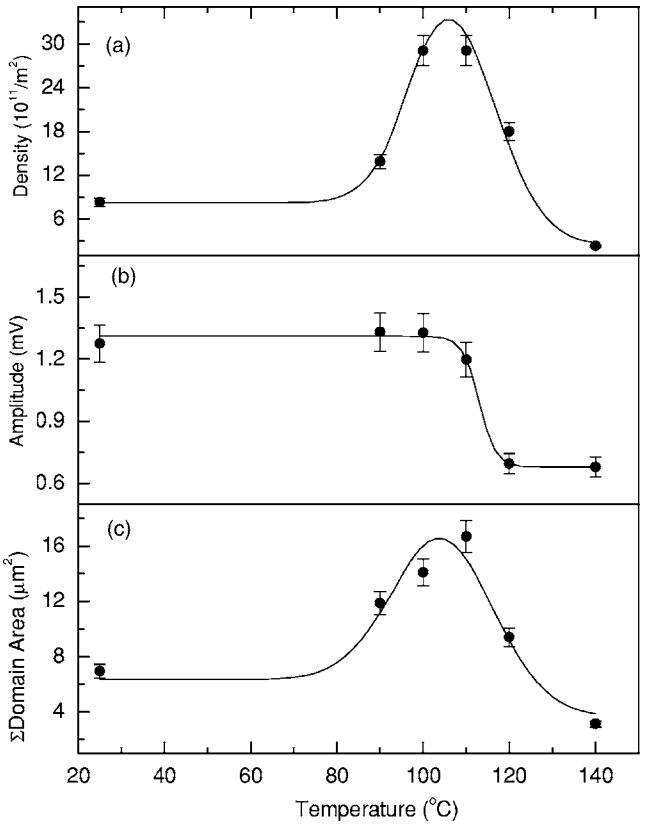

FIG. 8. Temperature dependence of (a) the domain density, (b) the average amplitude of piezoresponse, and (c) the sum of the domain areas of the poled (110)-cut PMN-25PT single crystal.

perature as shown in Fig. 5(f), an outlined region in Fig. 7(g) is magnified. A similar speckle-shaped domain pattern can be seen in Fig. 7(h) compared to that shown in Fig. 5(f), although the domain densities and shapes are not exactly the same.

In order to understand the detail of the newly appearing domains, analyses of the temperature dependence of the domain density, the average piezoresponse amplitude and the sum of the domain areas in the region outlined in Fig. 7(a) were illustrated in Fig. 8. There are a few points related to Figs. 7 and 8 that need to be noted. First, a domain wall expansion during heating is apparent for the "white" domains shown in Figs. 7(a)–7(c). This can be understood by the fact that new domains tend to nucleate at the domain walls due to the relatively low domain wall energy. However, the piezoresponse does not increase, although the domain wall expands during heating. Second, in contrast to those in the as-grown sample, both the domain density and the sum of the domain areas in the poled sample increase near T_m, corresponding to the newly appeared "white" dots in Fig. 7(b). Third, when the temperature is higher than T_m, PMN-25PT changes to a paraelectric phase; therefore, no obvious domain contrast can be observed as shown in Fig. 7(f) and the three analysis values have the same tendency as those observed in the as-grown sample.

IV. CONCLUSION

The study of ferroelectric domain structures and temperature-dependent domain evolution in poled and as-grown (110)-cut PMN-25PT single crystals revealed the following results: The as-grown PMN-25PT exhibits speckle-shaped microdomains with domain sizes ranging from less than 100 nm^2 to 8 μm^2, and the domain size distribution decreases exponentially as domain size increases. During the heating process from room temperature to approaching T_m, there is no obvious change in the density and the sum of areas of the microdomains, except the continuous decrease of the average piezoresponse amplitude. When temperature passed over T_m, the microdomains start to disappear, and when temperature is much higher than T_m, only PNRs retain, revealing the ferroelectricity in a broad temperature range. The speckle-shaped microdomains can be rebuilt by the random field in the cooling process. Stripe-shaped macrodomains with widths of around 10 μm were observed by the PFM in the (110)-cut and poled PMN-25PT single crystal. These macrodomains were found to undergo a transition to microdomains during heating to temperatures above 90 °C. Further heated to temperatures higher than the phase transition temperature of 115 °C, the microdomains finally disappear.

ACKNOWLEDGMENTS

The authors would like to thank W.W. Cao for stimulating discussions. This work was supported by the internal grant of the Hong Kong Polytechnic University (No. G-T855).

*Corresponding author. Electronic address: apdaijy@inet.polyu.edu.hk

[1] L. E. Cross, Ferroelectrics **76**, 241 (1987).
[2] D. Viehland, M. Wutting, and L. E. Cross, Ferroelectrics **123**, 71 (1991).
[3] V. Westphal, W. Kleemann, and M. D. Glinchuk, Phys. Rev. Lett. **68**, 847 (1992).
[4] O. Noblanc, P. Gaucher, and G. Calvarin, J. Appl. Phys. **79**, 4291 (1996).
[5] X. Y. Zhao, J. Wang, H. L. W. Chan, C. L. Choy, and H. S. Luo, Appl. Phys. A: Mater. Sci. Process. **80**, 653 (2005).
[6] Y. P. Guo, H. S. Luo, K. P. Chen, H. Q. Xu, X. W. Zhang, and Z. W. Yin, J. Appl. Phys. **92**, 6134 (2002).
[7] G. A. Samara, E. L. Venturini, and V. H. Schmidt, Phys. Rev. B **63**, 184104 (2001).
[8] G. A. Smolensky, J. Phys. Soc. Jpn. **28**, 26 (1970).
[9] G. Burns and F. H. Dacol, Phys. Rev. B **28**, 2527 (1983); Solid State Commun. **48**, 853 (1983).
[10] P. M. Gehring, S.-E. Park, and G. Shirane, Phys. Rev. Lett. **84**, 5216 (2000).
[11] T. Y. Koo, P. M. Gehring, G. Shirane, V. Kiryukhin, S.-G. Lee, and S.-W. Cheong, Phys. Rev. B **65**, 144113 (2002).

[12] S. Wakimoto, C. Stock, R. J. Birgeneau, Z.-G. Ye, W. Chen, W. J. L. Buyers, P. M. Gehring, and G. Shirane, Phys. Rev. B **65**, 172105 (2002).
[13] R. Blinc, J. Dolinsek, A. Gregorovic, B. Zalar, C. Filipic, Z. Kutnjak, A. Levstik, and R. Pirc, Phys. Rev. Lett. **83**, 424 (1999).
[14] R. Pirc and R. Blinc, Phys. Rev. B **60**, 13470 (1999).
[15] X. Yao, Z. Chen, and L. E. Cross, J. Appl. Phys. **54**, 3399 (1983).
[16] S. M. Fan, J. W. He, and X. Yao, Ferroelectrics **77**, 181 (1988).
[17] Z. Yin, X. Chen, X. Song, and J. Feng, Ferroelectrics **87**, 85 (1988).
[18] X. Zhao, Ph.D. thesis, Shanghai Institute of Ceramics, Chinese Academy of Science (2004).
[19] Z.-G. Ye and M. Dong, J. Appl. Phys. **87**, 2312 (2000).
[20] C. S. Tu, C. L. Tsai, J. S. Chen, and V. H. Schmidt, Phys. Rev. B **65**, 104113 (2002).
[21] C.-S. Tu, V. H. Schmidt, I.-C. Shih, and R. Chien, Phys. Rev. B **67**, 020102(R), (2003).
[22] C.-S. Tu, L.-F. Chen, V. H. Schmidt, and C.-L. Tsai, Jpn. J. Appl. Phys., Part 1 **40**, 4118 (2001).
[23] C.-S. Tu, C.-L. Tsai, V. H. Schmidt, H. Luo, and Z. Yin, J. Appl. Phys. **89**, 7908 (2001).
[24] H. S. Luo, G. S. Xu, H. Q. Xu, P. C. Wang, and Z. W. Yin, Jpn. J. Appl. Phys., Part 1 **39**, 5581 (2000).
[25] I. K. Bdikin, V. V. Shvartsman, and K. Kholkin, Appl. Phys. Lett. **83**, 4232 (2003).
[26] V. V. Shvartsman and A. L. Kholkin, Phys. Rev. B **69**, 014102 (2004).
[27] P. Lehnen, W. Kleemann, T. Woike, and R. Pankrath, Phys. Rev. B **64**, 224109 (2001).
[28] X. Zhao, J. Wang, Z. Peng, H. L. W. Chan, C. L. Choy, and H. Luo, Mater. Res. Bull. **39**, 223 (2004).
[29] Z. Feng, H. Luo, Y. Guo, T. He, and H. Xu, Solid State Commun. **126**, 347 (2003).
[30] X. Wan, H. Luo, J. Wang, H. L. W. Chan, and C. L. Choy, Solid State Commun. **129**, 401 (2004).
[31] Z.-G. Ye, Y. Bing, J. Gao, A. A. Bokov, P. Stephens, B. Noheda, and G. Shirane, Phys. Rev. B **67**, 104104 (2003).